Available online at www.sciencedirect.com

SciVerse ScienceDirect

Proceedings of the Combustion Institute 34 (2013) 1677–1685

Proceedings of the Combustion Institute

www.elsevier.com/locate/proci

Laser sheet dropsizing of evaporating sprays using simultaneous LIEF/MIE techniques

Wei Zeng, Min Xu *, Yuyin Zhang, Zhenkan Wang

School of Mechanical Engineering, Shanghai Jiao Tong University, National Engineering Laboratory for Automotive Electronic Control Technology, Shanghai 200240, China

Available online 11 August 2012

Abstract

Laser-induced-fluorescence/Mie-scattering (LIF/MIE) was proven to be a useful diagnostic for Sauter Mean Diameter (SMD) measurements in non-evaporating sprays. However, the measurement is not reliable for cases of an evaporating spray due to the interference of the fluorescence signal from the vapor phase. In this work, simultaneous Laser-induced-exciplex-fluorescence/Mie-scattering (LIEF/MIE) imaging techniques were proposed to obtain the SMD distribution of evaporating sprays. A special experimental condition was used to generate the flash-evaporating spray, which includes a fuel temperature of 60 °C and an ambient pressure of 20 kPa. Different from the conventional LIF/MIE technique, the combination of LIEF and Mie techniques allows eliminating the effect of tracer fluorescence from vapor phase in an evaporating spray. In addition, carefully selected tracers and specially designed filters were used to decrease the effects of variation on tracer concentration and temperature dependency of fluorescence intensity during evaporation. The numerical analysis based on geometrical optics approximation (GOA) and experimental analysis was conducted to determine the calibration coefficient K. Finally, SMD distribution of an evaporating spray measured by both LIEF/MIE and conventional LIF/MIE techniques was compared to PDI measurement. The results show that the SMD of the flash boiling spray obtained from LIEF/MIE is very close to those measured by PDI, while the results measured by LIF/MIE and PDI show a large deviation of around 40%. It indicates that the evaporation effect cannot be ignored for evaporating sprays.

Keywords: Laser sheet dropsizing; LIEF/MIE; Evaporating spray; Numerical and experimental analysis

1. Introduction

The Laser Sheet Dropsizing (LSD, also called LIF/MIE) is a method to determine the two-dimensional droplets size distribution in a spray [1]. Different from the point-wise measurement technique, such as the Phase Doppler Interferometry (PDI), the LSD technique has the ability to quantify temporal and spatial fluctuation of spray droplet size distribution, which is important to the engine combustion efficiency since it can influence the local air/fuel ratio.

The principle of the LSD technique relies on the assumption that the fluorescence intensity emitted by the fluorescent dye is proportional to the volume (d^3) of the droplet and that the

* Corresponding author. Address: Institute of Automotive Engineering, Shanghai Jiao Tong University, Shanghai 200240, China. Fax: +86 21 3420 6670.

E-mail addresses: wei.g.zeng@gmail.com (W. Zeng), mxu@sjtu.edu.cn (M. Xu).

1540-7489/$ - see front matter © 2012 The Combustion Institute. Published by Elsevier Inc. All rights reserved.
http://dx.doi.org/10.1016/j.proci.2012.07.061

scattered light intensity is proportional to its surface area (d^2) [2]. The ratio of the two intensity distribution on an illuminated plane of a spray is proportional to the Sauter Mean Diameter (SMD) and can be estimated, according to [3]

$$\mathrm{SMD} = \frac{1}{K} \cdot \frac{\int_{D=0}^{\infty} I_f(D) \cdot dN(D)}{\int_{D=0}^{\infty} I_s(D) \cdot dN(D)} \quad (1)$$

where I_f is the fluorescence intensity, I_s is the scattered light intensity, $dN(D)$ is the probability distribution of the spray droplets, K is the calibration coefficient.

The LIF/MIE technique was evaluated theoretically and experimentally by previous studies [4–7], suggesting some approaches to improve the accuracy of LIF/MIE measurement in sprays. While these studies show good results in the relatively dilute part of non-evaporating sprays [2,4], care must be taken in evaporating systems due to potential tracer fluorescence from the vapor phase, local and temporal variation of tracer concentration and temperature dependent fluorescence cross sections [1]. Since many of the real engine sprays have a high evaporation rate, new technology breakthroughs are necessary for improving the LSD accuracy on evaporating sprays. On the other hand, the effects of multiple-scattering on LIF and Mie signals lead to uncertainties of LSD measurement [8]. Focusing on a dilute region is a choice to decrease the effect of multiple-scattering. Combining with the SLIPI technique [9] would be an efficient way to remove issues caused by the multiple-scattering effect.

In this work, simultaneous Laser-induced-exciplex-fluorescence/Mie-scattering (LIEF/MIE) techniques were applied to obtain the quantitative SMD distribution of dilute region of evaporating sprays for the first time. The theoretical and experimental analysis was extended to enhance the sizing accuracy of the LIEF/MIE technique.

2. Experimental and theoretical approaches

2.1. LIEF/MIE technique for evaporating sprays

Different from the LIF/MIE technique, the combination of LIEF and Mie techniques allows eliminating the effect of tracer fluorescence from vapor phase for evaporating sprays. It also can decrease the effects of variation of tracer concentration and temperature dependent fluorescence by using specially designed exciplex system and carefully selected filters. LIEF technique was proposed by Melton [10] in 1980s which allows spectral separation of the liquid and vapor phase fluorescence signals by adding a tracer pair into a non-fluorescing base fuel. An organic additive which is the so-called monomer (M) is doped into the base fuel together at low concentration with another additive, known as the exciplex forming component (G). The monomer fluorescence is dominated in the vapor phase, while the exciplex fluorescence can be used to track the liquid phase. The detailed information of LIEF technique can be found in Refs. [11–14].

Practical application of LIEF/MIE technique needs to specially design the exciplex system. The selected exciplex mixture needs to have similar properties with actual fuel and the tracers need to co-evaporate with the base fuel so that the effect of tracer concentration variation can be decreased. The fluorobenzene(FB)/diethylmethylamine(DEMA)/*n*-hexane exciplex system is selected in this study since it has shown good co-evaporation based on components measurement of an evaporating droplet [12]. In FB/DEMA/*n*-hexane system, FB is the monomer (M), DEMA is the exciplex forming component (G) and *n*-hexane is the base fuel. The proportion of each component in FB/DEMA/*n*-hexane system is important to the LIEF/MIE measurement, which is determined by a theoretical method, as described below.

A laser sheet at 266 nm wavelength was used as the incident light. The liquid and vapor spectrum under 266 nm excitation is shown in Fig. 1. The liquid phase fluorescence signal and Mie-scattering signal are separated by two optical band-pass filters. The centerline wavelength/band-width for liquid phase fluorescence signal is 340 ± 10 nm. This filter is selected to decrease the effect of temperature dependent fluorescence intensity on LSD result, since the temperature sensitivity in this wavelength region is relatively low while the overall fluorescence intensity is high, according to Düwel's study [12]. The statements in this study show that the variation of fluorescence intensity from the 340 ± 10 filter is less than 7% when the temperature increases from 10 to 60 °C. The centerline wavelength/band-width for Mie-scattering signal is 266 ± 10 nm.

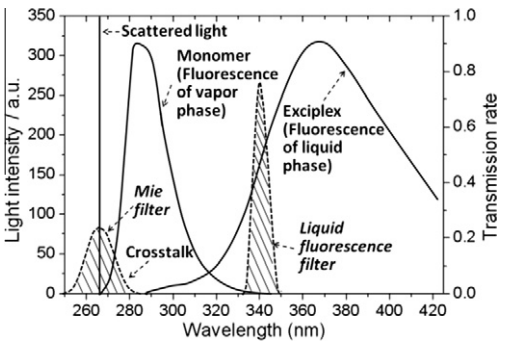

Fig. 1. Liquid and vapor spectrum under 266 nm excitation.

2.2. Theoretical method

To provide a accurate LSD measurement, the relation between scattered intensity and the surface area of the sphere is required to be d^2 dependence and the relation between fluorescence intensity and the volume of the sphere is required be d^3 dependence. These dependences were evaluated theoretically by Domann et al. [15–17], indicating that deviations of the emitted fluorescent light and the scattered light intensity from the assumed cubic and square droplet diameter could occur. The deviations were mostly caused by the attenuation of laser light within the droplet volume due to the dye absorption. Therefore, this study applied the theoretical method proposed by Domann et al. [2] to determine the dye concentration.

The theoretical approach is based on the geometrical optics approximation (GOA) that was originally developed by van de Hulst [18]. The GOA method is based on tracing the paths of a light from an incident laser beam through a single spherical droplet. The intensity of the light scattered by a sphere located in a single laser beam was calculated with proper account of the phases between surface reflection, refraction, 1st and 2nd internal reflections. The approach has been successfully compared with Mie theory [15]. It also showed that the GOA results agree with the experimental results well, indicating that the 3rd and higher order internal reflections only induce very small errors.

The GOA approach was extended to droplet with fluorescing dye by taking into account the light absorption along the paths of the light within the droplet. According to Guilbault [19], the fluorescence intensity emitted due to absorption over a specific path-length b within a liquid of dye concentration c is denoted by Eq. (2). This term comprises the intensity i_0 at the beginning of the absorbing, the quantum field φ and the molar extinction cross-section ε. In this study, the φ was fitted to a constant since the temperature variation is relatively small. Therefore, Eq. (2) only provides a relative value of the fluorescence intensity:

$$i_f = \phi \cdot i_0 \cdot (1 - e^{sbc}) \tag{2}$$

The dye absorption depends on the absorption coefficient, which is determined by the product of molar-extinction-cross-section and dye concentration. In the FB/DEMA/*n*-hexane system, DEMA is provided in excess concentration to maximally enhance the exciplex formation probability and it cannot absorb the incident light [13]. Therefore, the absorption of FB/DEMA/*n*-hexane mixture depends on FB. The molar-extinction-cross-section of FB is a constant of 10 m^2/mol [12]. The concentration of DEMA used in this study is a constant volume-percentage of 9%. Various FB concentrations are examined by calculations, namely 0.02%, 0.2%, 2% and 10%, corresponding to absorption coefficients of 0.00001, 0.0001, 0.001 and 0.005 mm^{-1}. The purpose of the calculations is to obtain the trade-off between the signal-to-noise ratio and the deviations of the fluorescent and scattered light intensities from the assumed cubic and square droplet diameter. Corresponding to different FB concentrations, the refractive index of the mixture varies from 1.375 to 1.38 which shows a negligible variation. The light collection angle for LSD experiment is from 89° to 91°.

The overall scattered and fluorescence intensities were calculated from the GOA approach from all the droplets present in various droplet size distributions with known Sauter Mean Diameters. Calculations were performed for many droplet size distributions, determined according to the Rosin–Rammler distribution function [2]:

$$1 - Q = \exp(1 - (D/x)^q) \tag{3}$$

where Q is the fraction of the total volume of the liquid carried by droplet diameters smaller than D. q and x are variables associated with the spread of the size distribution and the most probable diameter.

The size distribution, estimated from Eq. (3), is a cumulative volume distribution and is converted into a droplet number density size distribution. The function parameters q and x were selected to obtain wide variation of the spread of droplet size distribution. At given SMD, shapes and spreading of the distribution lead to different calibration coefficients [16]. This induces uncertainties in the measurement. Therefore, the effects of spreading of the distribution on the calibration coefficient were analyzed. In this study, q ranges from 1 to 40 and x ranges from 5 to 145. A range of SMD from 10 to 160 μm was examined. The calculation was conducted using in-house code.

3. Measurements

The LSD technique and the PDI technique were applied to measure droplet sizes in a spray produced by a high-pressure eight-hole GDI injector, as shown in Fig. 2. A pulsed Nd:YAG laser at

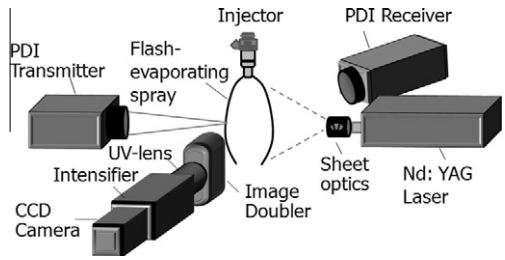

Fig. 2. Experiment setup for PDI and LSD.

Table 1
Experimental conditions.

Conditions	Injection pressure (MPa)	Ambient pressure (kPa)	Fuel temperature (°C)
1	2	100	20
2	5	100	20
3	10	100	20
4	10	20	60

266 nm was used to generate the laser sheet to illuminate the spray. Mie and LIEF images were captured simultaneously using an Image-Doubler, which was mounted in front of a UV-lens and an Intensifier-CCD camera. A PDI system was used in this study to measure the transient drop size characteristics. The test conditions are summarized in Table 1. The conditions 1–3 represent the non-evaporation cases, while the spray injected under condition 4 experiences flash-evaporating [20]. Since the collisional quenching by oxygen is one of the most stringent limitations of LIEF, all measurements were performed with nitrogen to avoid quenching by oxygen. The more detailed information of facilities and post-processing can be found in Ref. [20].

The spatial resolution of the LIEF/MIE technique is important. The test volume of PDI system is almost a cube of about $200 \times 200 \times 400$ μm (width × height × length). The thickness of laser sheet for LIEF/MIE measurement is about 500 μm, which is close to the length of PDI test volume. The physical pixel size of all LIEF/MIE images is a square of about 50×50 μm. Therefore, averaging over 16 pixels (4×4) was implemented for every LIEF/MIE image, resulting in an area of 200×200 μm which is consistent with the width × height of the PDI test volume.

More than 150 images were generated at first and the average value and standard deviation as a function of image number at each test condition were analyzed. As a consequence, the average value and standard deviation become constants when the image number is above 50. Thus, 50 images were used for post-processing at each condition.

4. Results and discussion

4.1. Theoretical evaluation

4.1.1. Determination of tracer concentration

The scattered intensity at the 90° scattering angle for the FB/DEMA/*n*-hexane mixture droplet is theoretically analyzed. To proceed with an evaluation of the SMD accuracy, the calculated intensity profiles are fitted to functions 4 and 5,

$$i_f = a_f \cdot D^{bf} \tag{4}$$

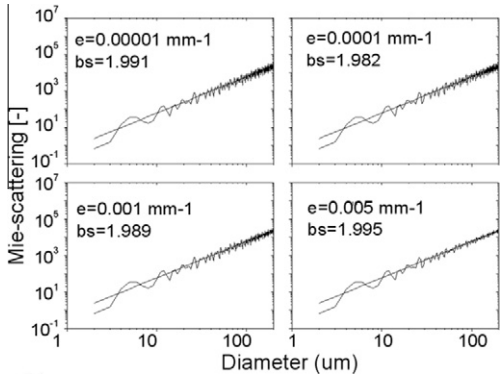

Fig. 3. Scattered intensity profiles under various absorption coefficients.

$$i_s = a_s \cdot D^{b_s} \tag{5}$$

where b_s and b_f are the exponents of the dependence of droplet diameter. Figure 3 shows scattered intensity profiles under various absorption coefficients. The fitting exponents (b_s) are 1.99, 1.98, 1.99 and 1.99, obtained from the plots of Fig. 3, corresponding to the various absorption coefficients. It shows that the fitting exponents are all within an acceptable deviation of the d^2 proportionality, where the maximal deviation is 0.9%. The dye absorption has a very small effect on the index of Mie-scattering intensity (b_s) at the 90° scattering angle for the FB/DEMA/*n*-hexane mixture. However, the profiles in Fig. 3 also show considerable oscillations due to interference of the surface reflection and the 2nd internal reflection.

Figure 4a shows profiles of relative fluorescence intensity as function of droplet diameter under various absorption coefficients. Figure 4b shows the fitting exponents obtained from plots of Fig. 4a under different diameter ranges. It provides the guideline for the selection of the fluorescence tracer and the corresponding concentration using the absorption coefficient. In the relative low absorption cases (0.00001 and 0.0001), the linear profile with exponent $b_f = 3$ over the entire diameter range is observed, indicating an ideal proportionality of intensity to droplet volume. At the case of 0.001 mm^{-1}, the fitting exponent b_f is 2.97 when the droplet diameter ranges from 0 to 160 μm, which is within an acceptable deviation (1%) of the d^3 proportionality. With larger absorption coefficients or larger diameters, the impact of light absorption increases continuously. The light extinction starts along one of the paths of refraction, 1st and 2nd internal reflections so that fluorescence is not generated over the complete distance of all paths. This leads to the transition from $b_f = 3$.

The GDI spray droplet size is usually less than 160 μm. Therefore, to obtain the trade-off between the signal-to-noise-ratio and the

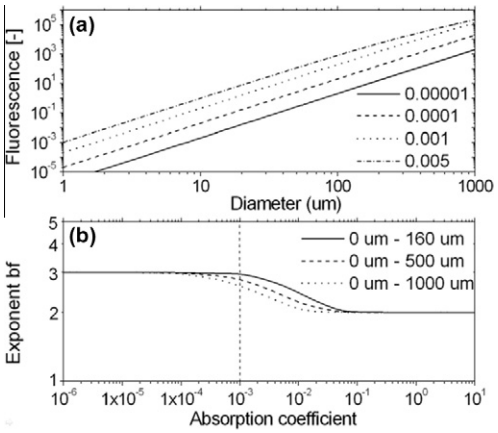

Fig. 4. Profiles of fluorescence intensity and corresponding values of b_f.

deviation of the fluorescent intensity from the cubic droplet diameter, the 2% FB concentration was selected, corresponding to the dye absorption coefficient of 0.001 mm^{-1}.

4.1.2. Calibration coefficient K under various droplet size distributions

The overall scattered and fluorescence intensities were estimated from all the droplets present in various droplet size distributions, determined according to the Rosin–Rammler function, as described above. The SMD of all droplets present in each droplet size distribution is calculated based on Eq. (6),

$$\mathrm{SMD} = \frac{\sum_{i=0}^{n} D_i^3}{\sum_{i=0}^{n} D_i^2} \tag{6}$$

where D is the droplet diameter. Then the calibration coefficient K is calculated using Eq. (1). Figure 5 presents the calculated value of the calibration coefficient K as a function of SMD. These are also relative values since the relative value of the fluorescence intensity is used. The continuous curve is a polynomial fit on the calculated values. The triangles in Fig. 5 represent the values of K for GDI spray droplet size distributions (q and x range from 3 to 6 and from 10 to 60, respectively). The stars indicate the values of K for mono-disperse distributions with different droplet diameters and the empty square represent a poly-disperse distribution that is comprised of all mono-disperse distributions. The filled circle represents the values of K for a wide range of distributions (q and x range from 1 to 40 and from 5 to 145, respectively).

The value of K varies with SMD. According to the trend of continuous curve, the value of K increases with increase in SMD when the SMD is smaller than around 30 μm. However, large deviations can be observed for the mono-disperse

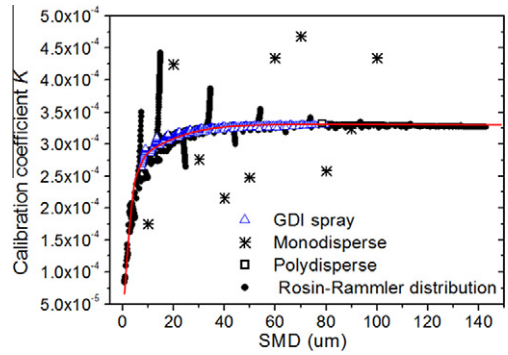

Fig. 5. Values of calculated calibration coefficient K versus SMD.

distributions. It can be clearly observed that the K values of mono-disperse distributions away from the continuous curve while the K value of poly-disperse distribution is fit on the curve. The reason is associated with large fluctuations of scattered light intensity, as analyzed above. However, since the GDI spray droplet size distributions are spread over a wide range of diameters and averaging over a sufficiently large number of droplets with a large size range mostly decreases the fluctuation effect, the K values of GDI spray droplet size distributions are well fit on the continuous curve with a maximum deviation of around 5%. A good polynomial correlation is observed between the SMD and the value of K for the droplet size distribution of GDI sprays. This result agrees with Ref. [2] for another tracer.

4.2. Calibration using PDI

To validate the theoretical correlation between SMD and calibration coefficient K for real GDI sprays, both LIEF/MIE and PDI measurements were conducted. The room-temperature conditions were selected to decrease the effect of fuel evaporation, including conditions 1–3 in Table 1. In this study, the PDI collection time began at 0 ms after the start of injection (SOI) and stopped at 10.0 ms after the SOI. The measurement points of PDI located at the center of spray plume at 40 and 50 mm downstream of the injector tip. The laser sheet images were taken for times between 1.0 and 5.0 ms after the SOI and the time step is 50 μs. Fifty images were recorded and accumulated at each time step.

Since the LSD is a technique to provide a snapshot of the spatial distribution while the PDI is a point-wise measurement technique, the conversion between the results of these two measurements is necessary before calculating the calibration coefficient K. Two data analyzing methods were proposed. In method one, the PDI data were used to calculate the SMD of all

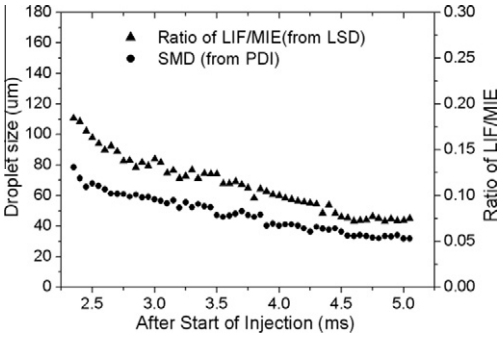

Fig. 6. Sauter Mean Diameters and the corresponding ratios of LIEF/MIE versus time at the center of the spray plume at 50 mm downstream of the injector tip under condition 1 (in method one).

droplets present in a narrow time period (30 μs) at a series of time step of collecting laser sheet images. The ratio of LIEF/MIE are obtained from the fluorescence and scattered light signals from sprays at the position of PDI measurement point at each time step. As an example, Fig. 6 shows the SMD and the corresponding ratio of LIEF/MIE as a function of ASOI. Then dividing the ratio of LIEF/MIE by the SMD derives a value of K at each time step. In method two, the SMD of all droplets present in a large time period (5 ms) were calculated using the PDI data. In the same time period, the fluorescence and scattered light signals from all sprays at the position of PDI measurement point were integrated to calculate the ratio of LIEF/MIE. Also, dividing the ratio of LIEF/MIE by the SMD derives the value of K.

Figure 7 presents the calibration coefficient K versus SMD for these two data analyzing methods, the experimental data from both methods agree with the theoretical results when the relative K obtained from calculation is multiplied by a carefully selected constant. The maximum deviation is less than 10%, indicating that the good correlation exists between the SMD and the calibration coefficient K for the real engine sprays. Therefore, this correlation can be used to correct the LSD results to enhance the sizing accuracy for real engine sprays.

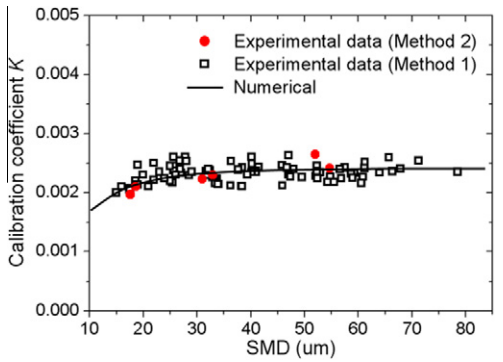

Fig. 7. Calibration coefficient K versus SMD.

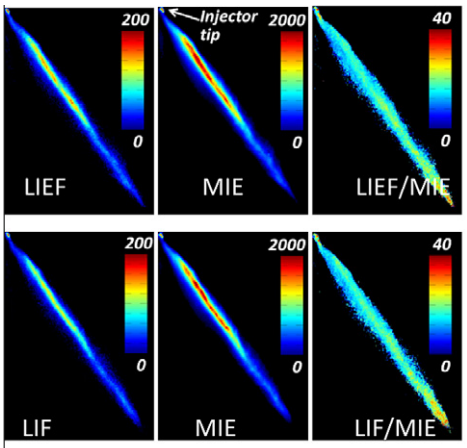

(a) Condition 1 (non-flash): 1.2 ms after start-of-injection (SOI), 10 MPa injection pressure, 20 °C fuel temperature and 100 kPa ambient pressure

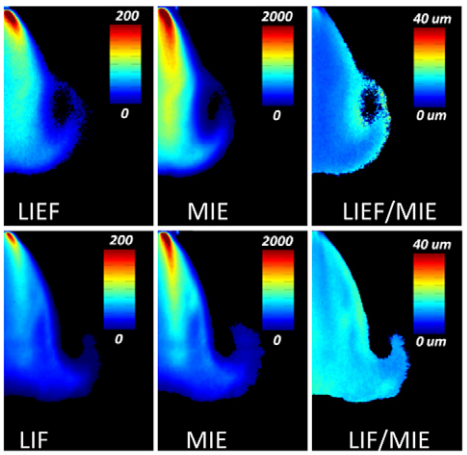

(b) Condition 2 (flash-evaporating): 1.2 ms after start-of-injection (SOI), 10 MPa injection pressure, 60 °C fuel temperature and 20 kPa ambient pressure

Fig. 8. Spray images obtained from LIEF/MIE and LIF/MIE measurements under conditions 4 and 5; all Mie-scattering and fluorescence images are average values of 50 single shots.

4.3. Sizing accuracy on flash-evaporating spray

Following appropriate choice of dye concentration and determination of calibration coefficient, the LIEF/MIE and the usual LIF/MIE techniques were applied to characterize both the

non-evaporating and evaporating sprays. For the usual LIF/MIE measurement, the centerline wavelength/band-width for Mie-scattering filter is still 266 ± 10 nm, while for fluorescence filter is 289 ± 10 nm. The test fuels for LIEF/MIE and LIF/MIE measurements are 2%FB/9%DEMA/89%*n*-hexane and 2%FB/98%*n*-hexane, respectively. Two test conditions were selected, including conditions 3 and 4 in Table 1. The evaporation of the spray generated under condition 4 is dominated by flare flash-boiling that the vapor diffusion rate is significantly lower than the evaporation rate [20]. The results of both LIEF/MIE and LIF/MIE techniques were compared to the results from PDI to examine the sizing accuracy.

Figure 8 presents the spray images obtained from LIEF/MIE and LIF/MIE measurements under conditions 3 and 4. The spray images provided in this study are at 1.2 ms after the start-of-injection and injection ending timing is 1.0 ms. Therefore, no more ligaments are present in the spray. The significant difference in spray structure between these two conditions is attributed to flash-boiling [20]. The evaporating spray shown in Fig. 8b is a fully flash-boiling spray. The spray structure of flash-boiling spray is very sensitive with the fuel saturation pressure. The saturation pressures of these two test fuels are slightly different so that spray structure is slightly changed.

Figure 9 shows the drop sizing results measured by LIEF/MIE, LIF/MIE and PDI at 40 and 50 mm downstream of injector tip. Data in both data analyzing methods are provided. At the non-evaporating case, the SMD results measured by LIEF/MIE, LIF/MIE and PDI agree with each other. At flare flash-boiling condition, quantitative SMD profiles measured by LIEF/MIE and PDI still show good agreement, while

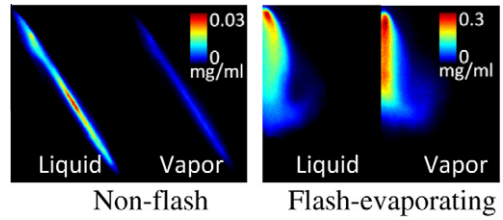

Fig. 10. Liquid and vapor phase images from the quantitative LIEF measurement [13]; images providing at 1.2 ms ASOI.

the results measured from LIF/MIE and PDI show a large deviation of around 40%. The SMD measured by LIF/MIE technique is larger than that by LIEF/MIE technique. The difference between LIEF/MIE and LIF/MIE results for the flash-boiling condition is anticipated to result from the effect of rapid evaporation. Previous LIEF measurements [13,20] for the 2%FB/9%DEMA/89%*n*-hexane mixture has provided individual structures of the liquid and vapor components, confirming this predication, as shown in Fig. 10. The vapor phase concentration at flash-evaporating condition is significantly larger than that at non-evaporating condition and the generated vapor phase is concentrated around the injector centerline. These indicate the rapid evaporation occurs in this condition. Therefore, the accurate measurement for evaporation sprays cannot be obtained by usual LIF/MIE technique due to the tracer fluorescence from the vapor phase, variation of tracer concentration and fluorescence intensity with temperature dependence.

The large difference between the results of LIEF/MIE and LIF/MIE measurements indicates that the evaporation effect cannot be ignored when spray experience strong-evaporation. The LIEF/

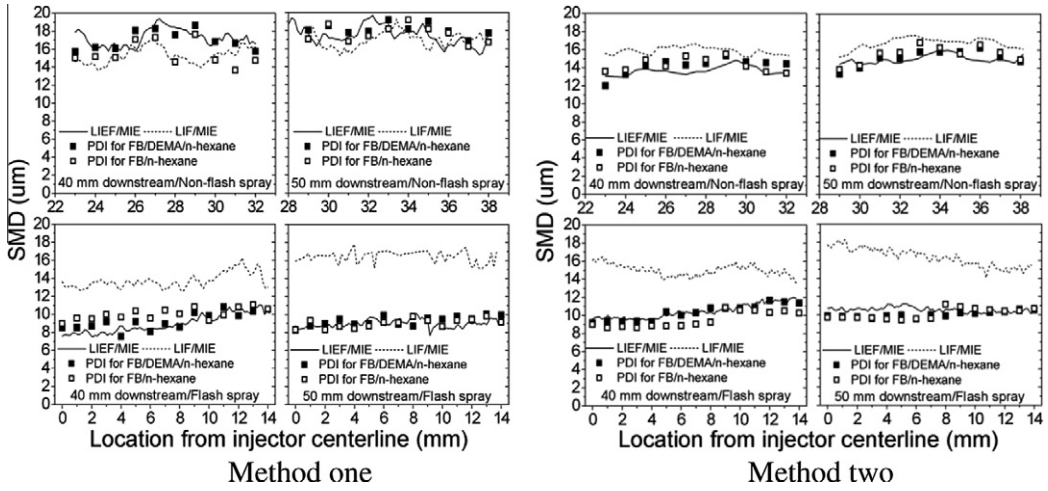

Fig. 9. Drop sizing results measured by LIEF/MIE, LIF/MIE and PDI at 40 and 50 mm downstream of injector tip.

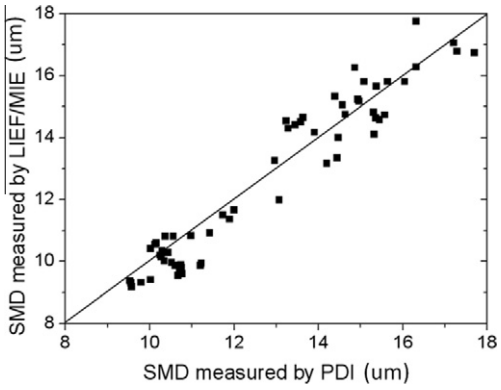

Fig. 11. Comparisons between LIEF/MIE and PDI results (in method one).

MIE technique and numerical approaches proposed in this study can provide a satisfied sizing accuracy for the dilute region (40 and 50 mm downstream) of evaporating sprays. Figure 11 presents the comparisons between calculated and measured SMD. The maximum deviation is about 14%. While some of the variance is attributed to measurement uncertainty related to the calibration of the technique against PDI, the oscillation of scattered intensity and the light absorption of the dye, the biggest unknown contribution is likely to be multiple scattering [4]. The LIEF/MIE results and PDI results show good agreement, indicating a relatively small multiple-scattering effect in the dilute region. However, it is important to understand the multiple-scattering effect when applying LIEF/MIE in the dense spray. The SLIPI technique is a possible solution to decrease the multiple-scattering effect [9].

Besides these effects, the uncertainty associated with temperature dependent fluorescence intensity is 7% as mentioned above. The variation associated with co-evaporation for mixture used in this study is 1.5% [12]. The effect of tracer fluorescence from the vapor phase can be ignored since the LIEF/MIE technique well separates the vapor phase from the liquid phase.

5. Conclusions

This study proposed the simultaneous LIEF/MIE laser sheet imaging technique for SMD measurement of evaporating sprays. The know-how for selection of the tracer concentration and determination of the calibration coefficient was given for the SMD measurement by using numerical and experimental analysis. Finally, SMD distribution of an evaporating spray measured by both LIEF/MIE and conventional LIF/MIE techniques was compared to PDI measurement. The conclusions are as follows:

(1) Both numerical and experimental results indicate that the calibration coefficient K varies with SMD. A good polynomial correlation is observed between the SMD and the value of K for the droplet size distribution of GDI sprays.
(2) For the non-evaporating spray, the SMD results measured by LIEF/MIE, LIF/MIE and PDI agree with each other. For evaporating spray, the SMD results measured by LIEF/MIE and PDI show good agreements, while the results measured by LIF/MIE and PDI show a large deviation of around 40%, indicating that the evaporation effect cannot be ignored.
(3) The maximum deviation between the results of LIEF/MIE and PDI is about 14%. It indicates that, by use of carefully selected tracers and specially designed filters, the LIEF/MIE technique combined with the numerical correction can provide a satisfied sizing accuracy for the dilute region of evaporating spray.
(4) Although the LIEF/MIE measurement shows an acceptable accuracy for evaporating sprays, caution should be taken when applying this technique to different sprays and fuel temperature conditions. In this case, the fluorescence tracers and filters need to be designed again.

Acknowledgements

The research was carried out at National Engineering Laboratory for Automotive Electronic Control Technology in Shanghai Jiao Tong University, and sponsored by Shanghai-Pujiang-Program (10PJ1406200), NSFC of China (51076093/E060702 and 51076090/E060404) and General Motors Company.

References

[1] I. Duwel, J. Schorr, J. Wolfrum, C. Schulz, *Appl. Phys. B* 78 (2) (2004) 127–131.
[2] R. Domann, Y. Hardalupas, *Part. Part. Syst. Charact.* 20 (2003) 209–218.
[3] Georgios Charalampous, Yannis Hardalupas, *Appl. Opt.* 50 (2011) 1197–1209.
[4] M.C. Jermy, D.A. Greenhalgh, *Appl. Phys. B* 71 (2000) 703–710.
[5] B.D. Stojkovic, V. Sick, *Appl. Phys. B* 73 (2001) 75–83.
[6] R. Domann, Y. Hardalupas, Eleventh International Symposium on Application of Laser Techniques to Fluid Mechanics, Lisbon, Portugal, 2002.
[7] J.W. Powell, C.F. Lee, *SAE paper* 2007-01-0648, 2007.
[8] E. Kristensson, L. Araneo, E. Berrocal, et al., *Opt. Express* 19 (2011) 13647–13663.

[9] E. Berrocal, E. Kristensson, M. Richter, M. Linne, M. Aldén, *Opt. Express* 16 (2008) 17870–17881.
[10] L.A. Melton, *Appl. Opt.* 22 (1983) 2224–2226.
[11] T.D. Fansler, M.C. Drake, B. Gajdeczko, et al., *Meas. Sci. Technol.* 20 (12) (2009) 125401.
[12] I. Düwel, W. Koban, F.P. Zimmermann, T. Dreier, C. Schulz, *Appl. Phys. B* 97 (2009) 909–918.
[13] G. Zhang, M. Xu, Y. Zhang, W. Zeng, *SAE paper* 2011-01-1879, 2011.
[14] P. Wieske, S. Wissel, G. Grünefeld, S. Pischinger, *Appl. Phys. B* 83 (2006) 323–329.
[15] R. Domann, Y. Hardalupas, A.R. Jones, *Meas. Sci. Technol.* 13 (2002) 280–291.
[16] G. Charalampous, Y. Hardalupas, *Appl. Opt.* 50 (9) (2011) 3622–3637.
[17] R. Domann, Y. Hardalupas, *Part. Part. Syst. Charact.* 18 (2001) 3–11.
[18] H.C. van de Hulst, *Light Scattering by Small Particles*, Dover, New York, 1981.
[19] C.G. Guilbault, *Practical Fluorescence–Theory, Methods and Techniques*, Marcel Dekker, 1973.
[20] W. Zeng, M. Xu, G. Zhang, Y. Zhang, D. Cleary, *Fuel* 95 (2012) 287–297.